

Self-Interaction Correction in Water–Ion Clusters

Kamal Wagle,^{1, a)} Biswajit Santra,^{1, b)} Puskar Bhattarai,¹ Chandra Shahi,² Mark R. Pederson,³ Koblar A. Jackson,² and John P. Perdew^{1, 4}

¹⁾Department of Physics, Temple University, Philadelphia, Pennsylvania 19122, USA

²⁾Department of Physics, Central Michigan University, Mount Pleasant, MI, 48859, USA

³⁾Department of Physics, University of Texas at El Paso, El Paso, TX, 79968, USA

⁴⁾Department of Chemistry, Temple University, Philadelphia, Pennsylvania 19122, USA

(Dated: 29 December 2020)

We study the importance of self-interaction errors in density functional approximations for various water–ion clusters. We have employed the Fermi–Löwdin orbital self-interaction correction (FLOSIC) method in conjunction with LSDA, PBE, and SCAN to describe binding energies of hydrogen-bonded water–ion clusters, *i.e.*, water–hydronium, water–hydroxide, water–halide, as well as non-hydrogen-bonded water–alkali clusters. In the hydrogen-bonded water–ion clusters, the building blocks are linked by hydrogen atoms, although the links are much stronger and longer-ranged than the normal hydrogen bonds between water molecules, because the monopole on the ion interacts with both permanent and induced dipoles on the water molecules. We find that self-interaction errors overbind the hydrogen-bonded water–ion clusters and that FLOSIC reduces the error and brings the binding energies into closer agreement with higher-level calculations. The non-hydrogen-bonded water–alkali clusters are not significantly affected by self-interaction errors. Self-interaction corrected PBE predicts the lowest mean unsigned error in binding energies (≤ 50 meV/H₂O) for hydrogen-bonded water–ion clusters. Self-interaction errors are also largely dependent on the cluster size, and FLOSIC does not accurately capture the subtle variation in all clusters, indicating the need for further refinement.

I. INTRODUCTION

Interactions between ions and water molecules play a critical role in many areas of physical chemistry, including electrochemistry, environmental chemistry, and biochemistry. Such water–ion interactions primarily involve hydrogen bonds (HBs), which appear with a wider range of bond strength (0.2–1.5 eV/H₂O)¹ and can be much stronger than HBs within neutral water clusters². One of the most common ionic HBs occurs between water molecules and their self-ionized forms, *i.e.*, H₃O⁺ and OH[−], which are responsible for acid-base chemistry, proton transfer, etc. Despite a long history of research, the microscopic details of the mechanism behind the proton transfer dynamics is yet to be settled³. Other ions, including halide ions and alkali ions, form strong bonds with water, and these interactions are also crucial for biochemistry and electrochemistry⁴.

Understanding the molecular-scale structure and dynamics of aqueous ionic solutions requires concerted efforts from both experiments and computer simulations^{4–7}. Among the simulation methods, Kohn–Sham density functional theory (DFT)⁸ based *ab initio* molecular dynamics is widely used and has been crucial in finding ion-solvation shell structures, autoionization processes, proton transfer mechanisms, and simultaneously the details of the electronic structure^{9–16}. The gas-phase water–ion clusters are important to benchmark the energetics, to explore the potential energy surface, and to understand the nature of water–ion interactions by energy decomposition^{17–21}. In this work, we focus on the energetics of various gas-phase water–ion clusters.

Historically, the accuracy of describing HBs is not satisfac-

tory with the most commonly used DFT exchange–correlation (XC) functionals (see review in ref. 22 and references therein). The accuracy of DFT functionals for HBs is widely tested in neutral water clusters. One of the key failures of DFT is that common semi-local and hybrid XC functionals predict an incorrect energetic ordering of isomers of the water hexamer^{22,23}. The origin of this error is mainly due to the lack of non-local van der Waals (vdW) interactions in those functionals^{22,23}. The non-empirical strongly constrained and appropriately normed (SCAN)²⁴ meta-GGA functional, which satisfies all 17 exact physical constraints that a semi-local XC functional can satisfy and includes intermediate-range dispersion, reproduces the correct energetic ordering among the isomers of the water hexamer^{2,25}. The strength of HBs also suffers from the self-interaction error (SIE) in DFT, and like all semi-local functionals SCAN is not free of SIE. Typically, the HBs in neutral water clusters are too strong due to the SIE^{2,22}. The water–ion interactions are also affected by SIE, resulting in too strong binding energies of water–ion clusters with semi-local functionals^{17–21}.

Fixing errors in specific methods for systems containing anionic or cationic species is challenging since the degree of electron delocalization impacts the monopole–dipole and monopole induced dipole energies which change significantly if the size or placement of an excess charge containing species is incorrect due to either errors of the theory or the size of basis sets. Among the systems studied here, the molecular anions OH[−] and OH[−](H₂O) and the atomic anions F[−], Cl[−], and Br[−] cannot bind the full excess electron in LSDA, PBE, and SCAN at the basis-set limit, while the other systems can. The SIE of semi-local density functional approximations tends to excessively delocalize electron density, which is more severe in small negatively-charged ions and molecules²⁶, typically leading to non-negative values for the Kohn–Sham eigenvalue of the highest occupied molecular orbital (HOMO)²⁷. The binding of the extra electron in anionic systems is also de-

^{a)}Electronic mail: kamal.wagle@temple.edu

^{b)}Electronic mail: biswajit.santra@temple.edu

pendent on the choice of basis sets for electronic wavefunctions^{28–31}. A fully converged basis may predict that a fraction of the extra electron is lost to the continuum³², whereas, a localized moderate-sized basis can artificially confine the extra electron^{28–31}, or trap a fraction of it on another center³³. Thus, self-interaction correction (SIC) to XC functionals is essential to achieve an accurate description of the density and energies of negatively-charged systems.

Hybrid functionals can partially alleviate SIE and predict more accurate HBs than semi-local functionals^{22,34}. In comparison, the Perdew-Zunger (PZ) SIC approach offers a fully nonlocal orbital-by-orbital removal of electron self-interaction from local and semi-local XC functionals. The PZ SIC method aims at eliminating the source of SIE in any approximate XC functional: its imperfect cancellation between the electron-electron self-repulsion (Hartree) and the approximate self-XC energy for any one-electron density²⁶. Recently, the Fermi-Löwdin orbital self-interaction correction (FLOSIC)^{35,36} was introduced as an efficient and unitarily invariant approach for implementing PZ SIC that can be used in conjunction with any approximate XC functional. The computational effort in the FLOSIC method allows for its application to clusters that were inaccessible through previous implementations^{37,38} of PZ SIC. The FLOSIC methodology has been used to study properties of chemical and physical interest for a range of systems^{39–48} including water^{2,49–51}. It has been shown that PZ SIC applied with SCAN significantly reduces the overbinding of HBs in neutral water clusters, predicting binding energies in much closer agreement with the CCSD(T)-F12, and simultaneously retaining the correct energetic ordering among the water hexamer isomers². It is thus quite important to explore how PZ SIC in conjunction with SCAN or other functionals performs in water-ion interactions.

Here, we have studied the effect of removing SIE on three non-empirical XC functional approximations, namely the local spin-density approximation (LSDA), the generalized gradient approximation formulated by Perdew, Burke, Ernzerhof (PBE)⁵², and the SCAN meta-GGA functional²⁴, in predicting the binding energies of protonated water clusters $[\text{H}_3\text{O}^+(\text{H}_2\text{O})_n, n=1,2,3 \text{ and } 6]$, deprotonated water clusters $[\text{OH}^-(\text{H}_2\text{O})_n, n=1–6]$, water-halide ion clusters $[\text{X}^-(\text{H}_2\text{O})_n, \text{X}=(\text{F}, \text{Cl}, \text{Br}), n=1–2]$, and water-alkali ion clusters $[\text{M}^+(\text{H}_2\text{O})_n, \text{M}=(\text{Li}, \text{Na}, \text{K}), n=1–2]$. We have analyzed how first-order and second-order (density-driven) errors in water-ion clusters depend on SIE. We find that self-interaction errors overbind the hydrogen-bonded water-ion clusters, and that FLOSIC reduces the error and brings the binding energies into closer agreement with higher-level calculations. FLOSIC applied to PBE predicts the lowest mean error in binding energies ($\leq 50 \text{ meV}/\text{H}_2\text{O}$) for hydrogen-bonded water-ion clusters.

II. METHODOLOGY

A. DFT and FLOSIC Calculations

Here, all calculations with density functional approximations (DFA) and the corresponding FLOSIC applied functionals, FLOSIC-DFA, were performed with the all-electron FLOSIC code^{54,55}, which was developed from the parent NRLMOL density-functional code^{56–60}. The code uses contracted Gaussian-type orbitals as basis sets that are optimized for density functionals and referred to as the DFO⁶¹. We have performed systematic basis-set convergence tests by adding diffuse functions on top of the DFO basis set. The details regarding the construction of the diffuse functions and basis set convergence are discussed in the next section. We used the local-density approximation (LSDA) which consists of the Slater-Dirac exchange⁶² and Perdew-Wang 92⁶³ correlation functional, the semi-local PBE⁶⁴ and the SCAN²⁴ XC functionals. All calculations were done using an accurate integration grid⁵⁴. For calculations involving the SCAN functional, especially dense grids were used⁶⁵.

The FLOSIC methodology^{35,36} is based upon the original PZ-SIC²⁶ method. In this method, SIE is removed from an approximate functionals $E_{\text{xc}}^{\text{approx}}[n_{\uparrow}, n_{\downarrow}]$ orbital by orbital, as given by

$$E^{\text{PZ-SIC}} = E_{\text{xc}}^{\text{approx}}[n_{\uparrow}, n_{\downarrow}] - \sum_{i\sigma} (E_{\text{xc}}^{\text{approx}}[n_{i\sigma}, 0] + U[n_{i\sigma}]), \quad (1)$$

where $n_{i\sigma}$ is a single orbital density and $U[n_{i\sigma}]$ is the Hartree electrostatic energy of that one-electron density. The orbitals must be localized to make $E^{\text{PZ-SIC}}$ size-extensive^{26,66}. The search for sufficiently localized orbitals that minimize Eq. 1 becomes computationally efficient with Fermi-Orbitals (FOs)⁶⁶. The FOs^{67,68} are obtained as

$$F_{i\sigma}(\mathbf{r}) = \frac{\sum_j^{N_{\sigma}} \psi_{j\sigma}^*(\mathbf{a}_{i\sigma}) \psi_{j\sigma}(\mathbf{r})}{\sqrt{\sum_j^{N_{\sigma}} |\psi_{j\sigma}(\mathbf{a}_{i\sigma})|^2}}, \quad (2)$$

where N_{σ} is the number of electrons with spin σ . Each FO, $F_{i\sigma}(\mathbf{r})$, depends on a position vector, $\mathbf{a}_{i\sigma}$, called a Fermi-Orbital Descriptor (FOD), and the spin density constructed by any set of orthonormal orbitals, $\psi_{j\sigma}(\mathbf{r})$, that spans the occupied space. The localized FOs are normalized but not mutually orthogonal. The Löwdin method of symmetric orthogonalization⁶⁹ is then performed to obtain the orthonormal Fermi-Löwdin orbitals (FLOs).

We employed a fully self-consistent procedure³⁶ to minimize the FLOSIC-DFA total energy. The calculations were initialized with a set of guessed FODs⁷⁰ to obtain self-consistent FLOs and total energy using an energy tolerance of 10^{-7} Hartree. Then the FODs are updated using derivatives of total energy with respect to FOD positions^{71–73} and gradient optimization methods, starting from the scaled⁷⁴ limited memory Broyden-Fletcher-Goldfarb-Shanno (L-BFGS)^{75–78} and switching, if necessary, to the conjugate gradient. Then self-consistent FLOs are obtained

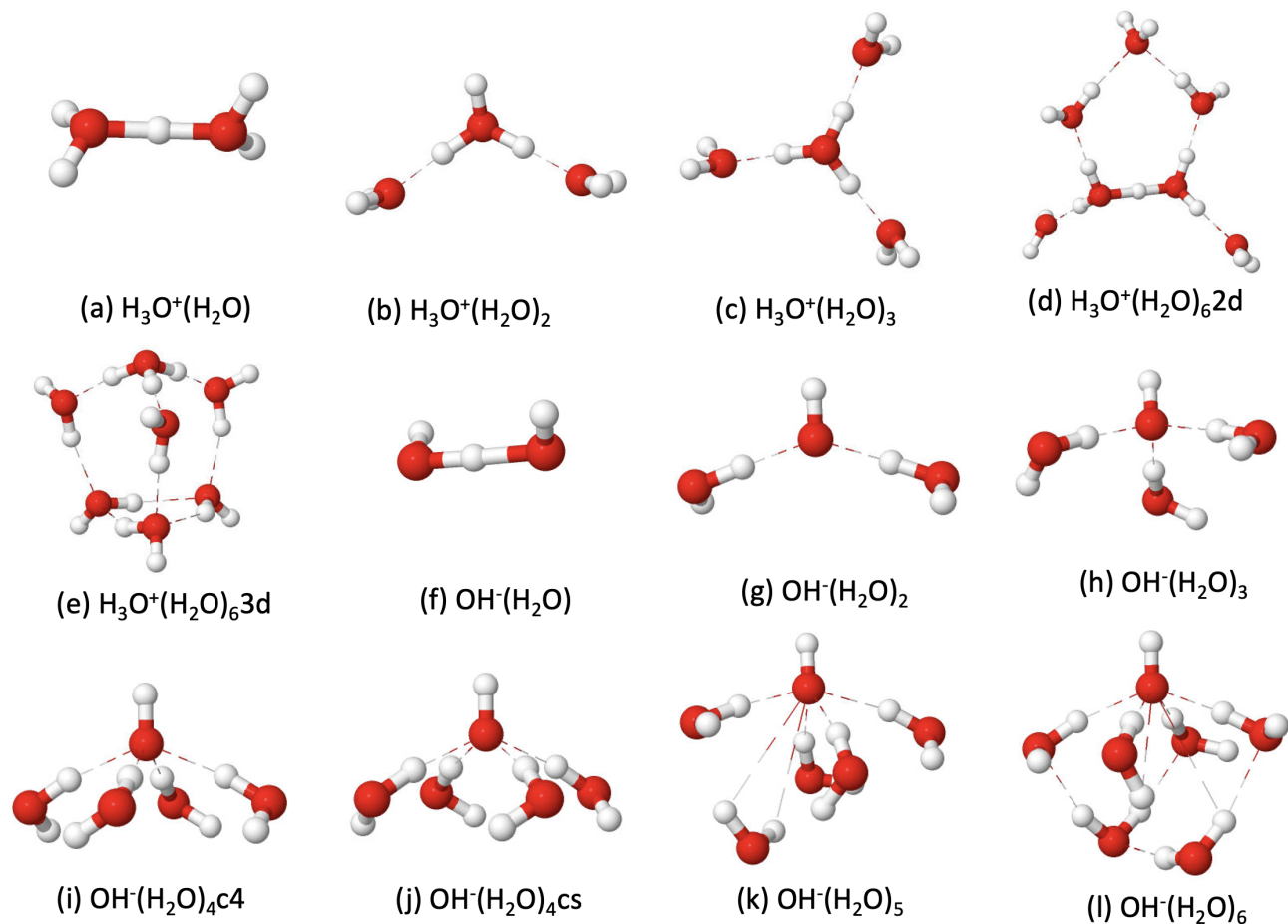


FIG. 1. Structures of protonated and deprotonated water clusters. Five protonated water clusters $\text{H}_3\text{O}^+(\text{H}_2\text{O})_n$ ($n = 1-3$, and 6) and seven deprotonated water clusters $\text{OH}^-(\text{H}_2\text{O})_n$ ($n = 1-6$) are taken from Ref. 53. The red and white spheres respectively indicate oxygen and hydrogen atoms. The dashed lines represent hydrogen-bonds.

with the new set of FODs. The iterative minimization of the total energy with respect to FODs is performed until the maximum FOD force component drops below 10^{-3} Hartree/Bohr.

We have also computed DFA energies on the corresponding FLOSIC-DFA self-interaction corrected density and FLOs, which is referred to as DFA@FLOSIC. The DFA@FLOSIC energies enable us to quantify the magnitude of the error in energy coming from a DFA density that suffers from self-interaction. The difference between DFA and DFA@FLOSIC energies is analogous to the commonly known density-driven-error^{79,80}. The Hartree-Fock density is often used to quantify the density-driven error since it is self-interaction (exchange only) free^{79,80}. The FLOSIC-DFA densities are self-interaction (exchange-correlation) free by definition.

B. Reference Geometry and Binding Energy

Fig. 1 shows structures of protonated and deprotonated clusters, which include five protonated water clusters $\text{H}_3\text{O}^+(\text{H}_2\text{O})_n$, $n=1-3$, and 6, and seven deprotonated water clusters $\text{OH}^-(\text{H}_2\text{O})_n$, $n=1-6$. The nuclear coordinates

of those clusters are taken from the WATER27⁵³ set which is part of the general main group thermochemistry, kinetics, and non-covalent interactions (GMTKN55)² benchmark database. The WATER27 geometries were optimized² at the B3LYP^{81,82}/6-311++G(2d,2p) level of theory. Fig. 2 shows the structures of water-halide and water-alkali clusters. We have considered six water-halide clusters $\text{X}^-(\text{H}_2\text{O})_n$ with $\text{X}=(\text{F}, \text{Cl}, \text{Br})$ and ($n=1$ and 2) and six water-alkali clusters $\text{M}^+(\text{H}_2\text{O})_n$ with $\text{M}=(\text{Li}, \text{Na}, \text{K})$ and ($n=1$ and 2). The nuclear coordinates of those clusters are taken from Ref. 17,21 which were optimized at the DF-MP2⁸³ level of theory with an aug-cc-pVTZ basis set.

For the clusters, the binding energy per water molecule (E_b) is defined as

$$E_b = \frac{E^{\text{cluster}} - nE^{\text{H}_2\text{O}} - E^{\text{ion}}}{n}, \quad (3)$$

where E^{cluster} is the total energy of a cluster that includes n H_2O molecules and one ion. $E^{\text{H}_2\text{O}}$ is the total energy of an isolated H_2O monomer at its equilibrium geometry and E^{ion} is the total energy of an isolated ion. E_b is negative for a stable cluster. Reference binding energies of protonated and depro-

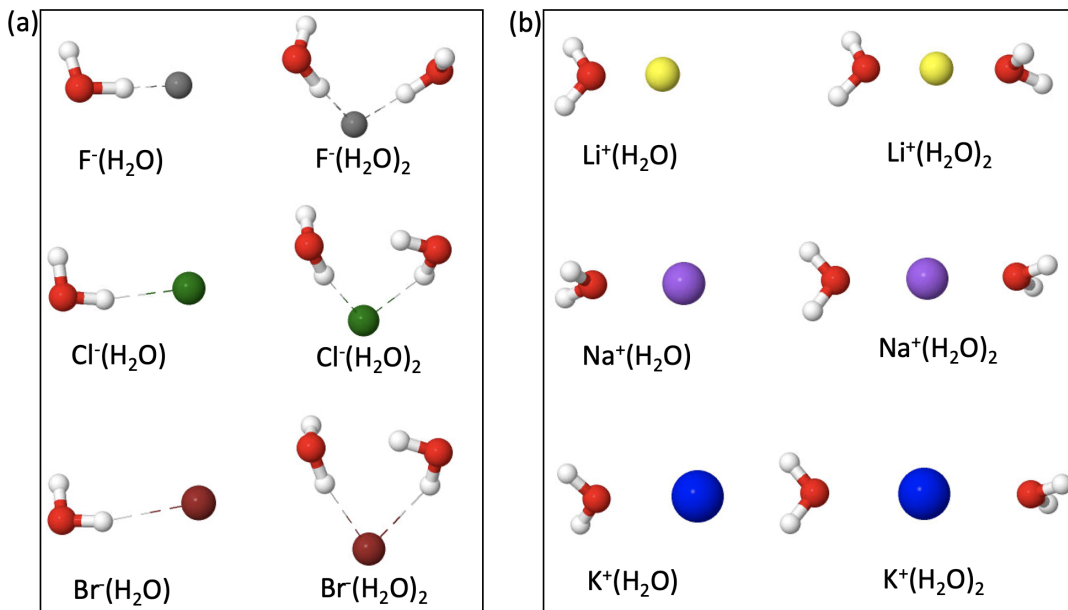


FIG. 2. Structures of the studied (a) water–halide clusters and (b) water–alkali clusters. Oxygen and hydrogen are represented by red and white spheres. The anions and cations are marked by other colors. Dashed lines represent hydrogen-bonding.

tonated water clusters were computed at the explicitly correlated coupled-cluster level of theory, CCSD(T)-F12b^{84,85}, at the complete basis set (CBS) limit, and are taken from Ref. 86. The reference binding energies with CCSD(T)-F12b at the CBS limit are taken from Ref. 17 for the water–halide and from Ref. 87 for the water–alkali clusters.

III. RESULTS AND DISCUSSIONS

A. Basis-Set and Density Error

Given that the semi-local functionals LSDA, PBE, and SCAN can bind only a fraction of the excess electron in the complete-basis-set limit as discussed in the introduction, we will use for those functionals basis sets without diffuse basis functions. Restricting the basis set is a familiar computational choice that makes the semi-local functionals look somewhat better than they are. The rest of this section will discuss the basis sets and their effects without and with self-interaction.

The erroneous delocalization of the extra electron in anions obtained with semi-local DFAs is dependent on the size of the basis set. On the one hand, the use of a moderate-sized localized basis can compensate for the delocalization. On the other hand, accurate description of HBs often requires a large basis with some diffuse Gaussian functions (*i.e.*, with relatively small exponents). The deprotonated water clusters are negatively charged and held together by HBs, for which the need for diffuse functions is ambiguous, and we explore this issue here. Fortunately, through the FLOSIC–DFA method we have electron densities of the negatively charged clusters that are free from self-interaction and that can be used to test the energy convergence with the size of the basis.

First, we briefly describe the basis sets we have used to determine the energy convergence. The NRLMOL DFO basis with standard additional polarization functions consists of $5s, 4p, 4d$ functions for O and $4s, 4p, 2d$ for H, which we refer to as DFO*. On top of the DFO* basis, we add diffuse functions of types s , p , and d for both O and H. The modified basis sets are defined as: i) *diffuse-1* which includes O(s) and H(s) diffuse functions, ii) *diffuse-2* which includes O(s, p) and H(s) diffuse functions, iii) *diffuse-3* which includes O(s, p) and H(s, p) diffuse functions, and iv) *diffuse-4* which includes O(s, p, d) and H(s, p) diffuse functions.

Fig. 3(a) shows the convergence of the total energy of OH^- with respect to an increasing number of diffuse basis functions. The energies are almost converged around the *diffuse-4* basis, and with respect to that, the energies obtained with DFO* differ by less than 1 mHa in both FLOSIC–PBE and FLOSIC–SCAN. In contrast, the two semi-local functionals show a much larger change in energy than their FLOSIC counterparts, and a significant portion of this discrepancy is due to erroneous density since PBE and SCAN energies computed at their corresponding self-interaction corrected densities, *i.e.*, PBE@FLOSIC and SCAN@FLOSIC, substantially reduce the discrepancy. For this small anion, in PBE or SCAN without SIC, a fraction of the excess electron would escape in the complete basis-set limit. Here we regard the difference between DFA energy computed at its self-consistent density and self-interaction free FLOSIC–DFA density as an estimate of the density-driven error. The density-driven error is quite significant in OH^- (where it could be even larger than we have estimated here) and is negligible in H_3O^+ and H_2O molecules. This indicates that extra diffuse functions can exaggerate the erroneous density delocalization in OH^- and a suitable choice of a converged basis is not straightforward for

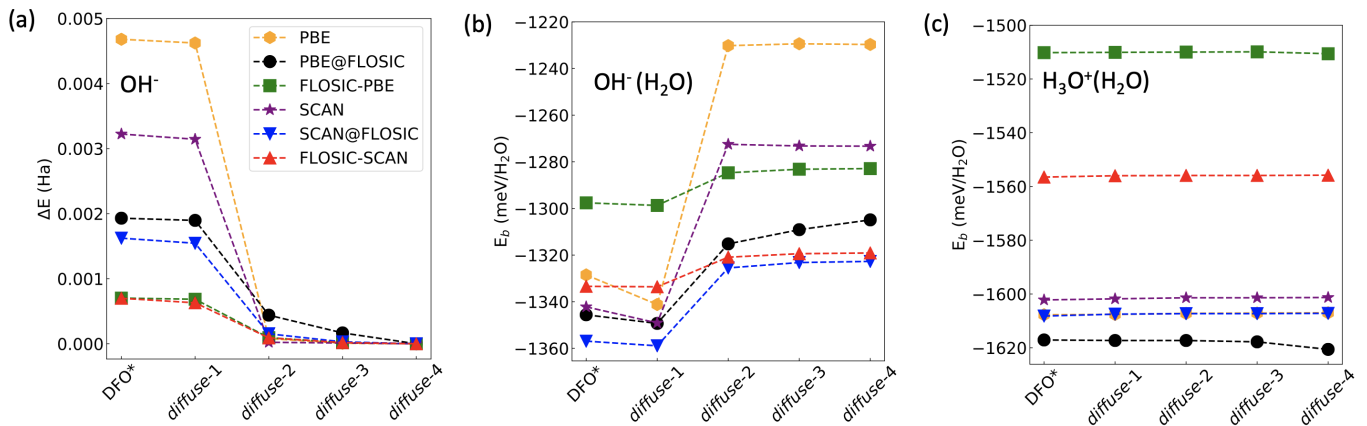


FIG. 3. (a) The basis-set dependence of the total energy of OH^- , plotted with respect to the *diffuse-4* basis (see text for the details of basis). Variation of the binding energy (E_b) of the (b) $\text{OH}^-(\text{H}_2\text{O})$ and (c) $\text{H}_3\text{O}^+(\text{H}_2\text{O})$ molecules with increasing size of the basis. Here DFA@FLOSIC refers to the DFA energy computed at the corresponding FLOSIC–DFA density. At the complete basis set limit, only SIC can bind the full excess electron in OH^- and $\text{OH}^-(\text{H}_2\text{O})$.

PBE and SCAN.

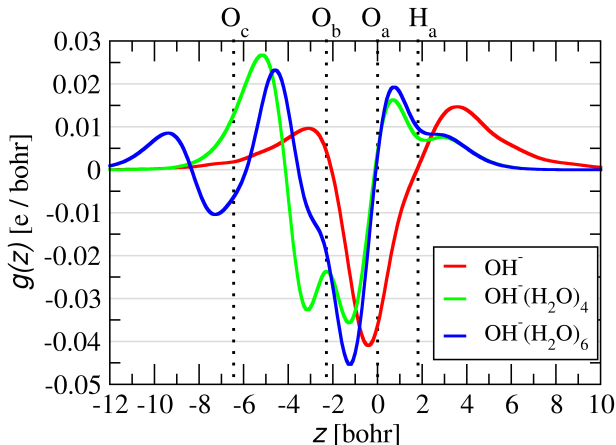


FIG. 4. Projection onto the OH^- axis of the PBE self-interaction error of the electron density for the hydroxyl group and two hydroxyl-water clusters. For further explanation, see the last two paragraphs of section 3.1.

TABLE I. Three measures of the size of the PBE self-interaction error of the electron density in hydroxyl-water clusters. For further explanation, see the last two paragraphs of section 3.1.

System	$\delta n_{z>0}$ (e)	$\delta \mu_z$ (D)	$ \delta \mu $ (D)
OH^-	0.026	0.37	0.37
$\text{OH}^-(\text{H}_2\text{O})_4$	0.042	-0.07	0.09
$\text{OH}^-(\text{H}_2\text{O})_6$	0.048	0.02	0.11

Fig. 3(b) shows the convergence of the binding energy of $\text{OH}^-(\text{H}_2\text{O})$ with respect to basis. From DFO* to *diffuse-3* basis E_b changes by ~ 14 meV/ H_2O with both FLOSIC–PBE and FLOSIC–SCAN, but the change is much larger with PBE (99 meV/ H_2O) and SCAN (69 meV/ H_2O). This

again shows that the addition of diffuse functions for negatively charged molecules can be problematic without SIC. The PBE@FLOSIC and SCAN@FLOSIC show a much smoother convergence of E_b , predicting, respectively, a 40 meV/ H_2O and 33 meV/ H_2O difference between the DFO* and *diffuse-3* basis. The density-driven error (*i.e.*, the difference between DFA and DFA@FLOSIC) in the binding of $\text{OH}^-(\text{H}_2\text{O})$ becomes much larger with additional diffuse functions, more so in PBE (76 meV/ H_2O) than in SCAN (51 meV/ H_2O) with the *diffuse-3* basis. In comparison, the E_b of $\text{H}_3\text{O}^+(\text{H}_2\text{O})$ shows very little (< 10 meV/ H_2O) density-driven error with and without the diffuse functions, as shown in Fig. 3(c). From Fig. 3(b) we conclude that PBE@FLOSIC and SCAN@FLOSIC binding energies are converged at the *diffuse-3* basis, which is similar to the convergence of the FLOSIC–DFAs. Also, Fig. 3(b) shows that the PBE (SCAN) energy at the DFO* basis are close to the PBE@FLOSIC (SCAN@FLOSIC) energy at the *diffuse-3* basis, indicating that the error due to a relatively smaller basis cancels to some extent with the density delocalization errors. In the following, we report and discuss results obtained with the DFO* for LSDA, PBE, and SCAN, and with the *diffuse-3* basis for all other functionals.

There will be a self-interaction (delocalization) error of the electron density from a density functional (*e.g.*, PBE) approximation, even in anion clusters like $\text{OH}^-(\text{H}_2\text{O})_{n \geq 2}$ that bind the full extra electron in the complete basis-set limit for that approximation. Here we will show that this error is rather small but systematic, at least up to $n=6$. Fig. 1 shows that the hydroxyl anion is found on the surface of each of these clusters. It could be interesting in future work to see if the delocalization error is larger in larger clusters or bulk, where the hydroxyl anion can be completely solvated by the waters.

For this purpose, we define the PBE self-interaction error of the density as $\delta n(\mathbf{r}) = n_{\text{PBE}}(\mathbf{r}) - n_{\text{FLOSIC-PBE}}(\mathbf{r})$, a function that integrates to zero electrons. To visualize this, we take the origin of coordinates on the O^- or O_a nucleus, and the z axis

pointing to the H or H_a nucleus of the hydroxyl group. Then we project $\delta n(\mathbf{r})$ onto the z axis via

$$g(z) = \int dx dy dz' \delta n(x, y, z') \frac{a}{\sqrt{\pi}} \exp -a^2(z' - z)^2, \quad (4)$$

where $a=1 \text{ bohr}^{-1}$ is large enough for atomic resolution and small enough for numerical real-space grids. The interpretation is that $\int_A^B dz g(z)$ is the PBE self-interaction error in the number of electrons between the planes $z = A$ and $z = B$.

Fig. 4 shows $g(z)$ for the hydroxyl anion and its bound complexes with four or six water molecules. The oxygens O_b on the four nearest-neighbor waters are located at approximately the same negative z , and those O_c on the two second-neighbor waters are located at a more negative z . (Average z coordinates for each set of neighboring oxygens are shown in Fig. 4) The PBE self-interaction error clearly removes a small fraction of an electron from each oxygen site, and transfers it to the hydrogen sites or to the surface (and in particular the ends) of the cluster. Table I shows the small fraction of an electron transferred into the half-space $z > 0$ ($\delta n_{z>0}$), and the corresponding small PBE self-interaction errors in the z component ($\delta \mu_z$) and magnitude of the dipole moment ($|\delta \mu|$). Note that the magnitudes of the dipole moment of OH^- in our calculation using PBE and FLOSIC–PBE are 0.58 Debye and 0.95 Debye, respectively. For comparison, the magnitudes of the dipole moment of an isolated water molecule are 1.79 Debye and 1.91 Debye, respectively from PBE and FLOSIC–PBE.

B. Deprotonated and Protonated Water Clusters

The hydroxide and hydronium ions form strong hydrogen bonds with water molecules. It can be seen from the reference⁸⁶ CCSD(T)/F12b energies that the binding energy of $\text{H}_3\text{O}^+(\text{H}_2\text{O})$ is stronger by 306 meV/ H_2O stronger than that of $\text{OH}^-(\text{H}_2\text{O})$ (Table II). In $\text{H}_3\text{O}^+(\text{H}_2\text{O})$, the shared proton sits exactly at the center between the two oxygen atoms separated by 2.40 Å (Fig. 1(a)), whereas, in $\text{OH}^-(\text{H}_2\text{O})$, the O-O distance is 2.47 Å, and the shared proton has one covalent O-H bond of length 1.12 Å and one hydrogen bond of length 1.34 Å. In the bigger clusters, the binding per molecule decreases due to relatively weak water–water interactions, $\sim 330 \text{ meV}/\text{H}_2\text{O}$ for $(\text{H}_2\text{O})_6^2$. With increasing cluster size, the binding per molecule gradually decreases, as explained at the end of the caption of Table 1. It is interesting that both $\text{H}_3\text{O}^+(\text{H}_2\text{O})_6$ and $\text{OH}^-(\text{H}_2\text{O})_6$ clusters become almost equally stable, differing by $< 15 \text{ meV}/\text{H}_2\text{O}$ with CCSD(T)/F12b. All of the studied XC functionals qualitatively reproduce the relative stability of these two types of clusters (Table II). However, there are non-negligible errors in the binding energy of an individual cluster obtained with all functionals. We explore the errors in more detail in Fig. 5, omitting the LSDA-based methods which provide errors $> 200 \text{ meV}/\text{H}_2\text{O}$.

Overall, it is evident from Fig. 5(a) and (b) that FLOSIC–PBE performs better than FLOSIC–SCAN for almost all of these clusters. The MUEs indicate that there is a systematic reduction in the error in binding energies with the

FLOSIC–DFA methods compared to the corresponding parent DFAs (Table II). For the deprotonated clusters, the MUE of FLOSIC–SCAN is 78 meV/ H_2O , reducing the MUE by 20 meV/ H_2O from SCAN@FLOSIC. For the protonated clusters, SCAN@FLOSIC and FLOSIC–SCAN predict MUEs of 85 meV/ H_2O and 46 meV/ H_2O , respectively. FLOSIC–PBE provides the best agreement with the reference binding energies in both types of clusters, predicting MUEs of 41 meV/ H_2O and 23 meV/ H_2O for deprotonated and protonated clusters, respectively. We find that our FLOSIC–PBE MUE for the deprotonated clusters is comparable to the hybrid functional PBE0/def2-QZVP mean error (31 meV/ H_2O) reported by Grimme and co-workers⁸⁸. In addition, the FLOSIC–PBE MUE for the protonated clusters is more accurate than the PBE0/def2-QZVP method (MUE of 44 meV/ H_2O)⁸⁸.

As shown in Figs. 5(a) and (b), the magnitude of the error in E_b decreases with increasing cluster size in all XC functionals. PBE@FLOSIC and SCAN@FLOSIC strongly overbind (by more than $\sim 150 \text{ meV}/\text{H}_2\text{O}$) the two small clusters, $\text{OH}^-(\text{H}_2\text{O})$ and $\text{H}_3\text{O}^+(\text{H}_2\text{O})$, and the errors tend to decrease in the larger clusters. PBE@FLOSIC performs better than SCAN@FLOSIC in the larger clusters, particularly in deprotonated clusters (Fig. 5(a)). We find that self-interaction corrections weaken the strength of HBs and result in more accurate binding energies than found with the uncorrected functionals. However, the accuracy of the self-interaction corrected functionals are inconsistent under variation of cluster size due to irregularities in the magnitude of the SIC to the binding of the clusters (E_b^{SIC}). The value of E_b^{SIC} is the difference between the FLOSIC–DFA and DFA@FLOSIC binding energies. As shown in Figs. 5(c) and (d), E_b^{SIC} from FLOSIC–PBE is $\sim 20 \text{ meV}/\text{H}_2\text{O}$ for the smallest as well as the largest deprotonated clusters, and it fluctuates in the range of 4–28 meV/ H_2O for the intermediate-sized clusters, without showing any clear trend with respect to cluster size (Fig. 5(c)). With FLOSIC–SCAN, E_b^{SIC} is exceptionally small (4 meV/ H_2O) in $\text{OH}^-(\text{H}_2\text{O})$. This is because the total SIC computed from the $\text{OH}^-(\text{H}_2\text{O})$ molecule largely cancels the sum of the SIC energies of the isolated H_2O and OH^- molecules. In contrast, E_b^{SIC} is much larger in $\text{H}_3\text{O}^+(\text{H}_2\text{O})$, *i.e.*, 109 meV/ H_2O and 52 meV/ H_2O with FLOSIC–PBE and FLOSIC–SCAN, respectively (Fig. 5(d)). E_b^{SIC} is reduced in both FLOSIC–PBE (19 meV/ H_2O) and FLOSIC–SCAN (30 meV/ H_2O) for the largest protonated cluster. These values are also similar to the E_b^{SIC} obtained in $\text{OH}^-(\text{H}_2\text{O})_6$. It is surprising that FLOSIC–SCAN provides too small E_b^{SIC} in $\text{OH}^-(\text{H}_2\text{O})$, as opposed to that in $\text{H}_3\text{O}^+(\text{H}_2\text{O})$. We explore this issue in more detail.

We note that the SIC energy obtained from each localized orbital (as given by the second term in Eq. (1)) with FLOSIC–SCAN is positive in these molecules, since for a given noded orbital density the SCAN XC energy is too negative compared to the exact XC energy (the negative of the Hartree energy). Since the SCAN total energy is already very accurate, this self-interaction “correction” from noded orbital densities actually worsens it⁴⁴. The SIC energy in each lone-pair orbital is greater than that in each bond-pair orbital by $\sim 35\%$ in the isolated OH^- , H_2O , and H_3O^+ molecules. Table III shows the decomposition of the total SIC energy into contributions from

TABLE II. Binding energies with density functionals and the corresponding mean unsigned errors (MUEs) computed with respect to the CCSD(T)-F12b reference⁸⁶ for deprotonated and protonated water clusters. The final column shows the percent error (PE) for FLOSIC–PBE. The energies are obtained with the basis DFO* for LSDA, PBE, and SCAN, and with *diffuse-3* for all other functionals. The corresponding reference value for the neutral $(\text{H}_2\text{O})_6$ prism is -332 meV/ H_2O , suggesting that the charged group is bound strongly to all the water molecules, as sketched in Fig. 1.

Cluster	Binding Energy (meV/ H_2O)										PE	
	Ref.	LSDA	LSDA@ FLOSIC	FLOSIC– LSDA	PBE	PBE@ FLOSIC	FLOSIC– PBE	SCAN	SCAN@ FLOSIC	FLOSIC– SCAN	FLOSIC– PBE	
$\text{OH}^-(\text{H}_2\text{O})$	-1157	-1646	-1631	-1504	-1329	-1305	-1283	-1342	-1324	-1319	-1319	10.9 %
$\text{OH}^-(\text{H}_2\text{O})_2$	-1056	-1408	-1399	-1299	-1147	-1136	-1108	-1176	-1168	-1147	-1147	5.0 %
$\text{OH}^-(\text{H}_2\text{O})_3$	-976	-1273	-1272	-1213	-1038	-1038	-1041	-1069	-1066	-1066	-1066	6.7 %
$\text{OH}^-(\text{H}_2\text{O})_{4c4}$	-915	-1175	-1170	-1106	-938	-937	-929	-992	-989	-967	-967	1.6 %
$\text{OH}^-(\text{H}_2\text{O})_{4cs}$	-922	-1235	-1229	-1147	-956	-954	-943	-1013	-1009	-982	-982	2.4 %
$\text{OH}^-(\text{H}_2\text{O})_5$	-874	-1168	-1160	-1078	-890	-888	-873	-955	-953	-921	-921	-0.1 %
$\text{OH}^-(\text{H}_2\text{O})_6$	-836	-1134	-1126	-1037	-854	-853	-833	-914	-912	-881	-881	-0.4 %
MUE	–	329	322	235	59	54	41	104	98	78	–	–
$\text{H}_3\text{O}^+(\text{H}_2\text{O})$	-1463	-1909	-1926	-1742	-1608	-1618	-1510	-1602	-1608	-1556	-1556	3.2 %
$\text{H}_3\text{O}^+(\text{H}_2\text{O})_2$	-1238	-1569	-1577	-1451	-1314	-1323	-1253	-1330	-1335	-1276	-1276	1.2 %
$\text{H}_3\text{O}^+(\text{H}_2\text{O})_3$	-1110	-1380	-1387	-1306	-1156	-1165	-1131	-1173	-1179	-1152	-1152	1.9 %
$\text{H}_3\text{O}^+(\text{H}_2\text{O})_{62d}$	-830	-1083	-1086	-1008	-865	-872	-843	-882	-885	-855	-855	1.6 %
$\text{H}_3\text{O}^+(\text{H}_2\text{O})_{63d}$	-851	-1127	-1129	-1051	-878	-887	-868	-908	-911	-881	-881	2.0 %
MUE	–	315	323	213	66	75	23	81	85	46	–	–

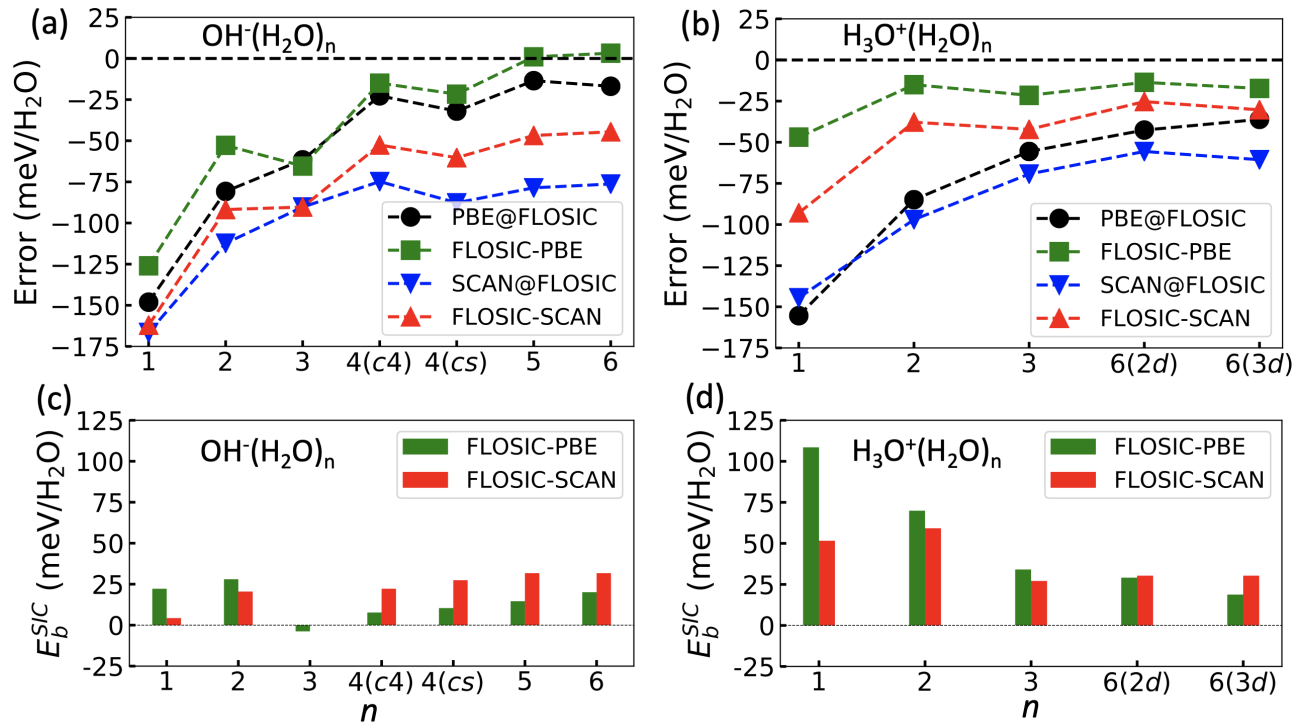


FIG. 5. Error in the binding energies of the (a) deprotonated water clusters $\text{OH}^-(\text{H}_2\text{O})_n$ ($n = 1-6$) and (b) protonated water clusters $\text{H}_3\text{O}^+(\text{H}_2\text{O})_n$ ($n = 1-3$, and 6) with various functionals compared to the CCSD(T)-F12b reference⁸⁶. Here a negative sign indicates overbinding. Self-interaction correction to the binding energies (E_b^{SIC}) of the (c) deprotonated and (d) protonated water clusters.

core, lone-pair, and bond-pair orbitals. The self-interaction correction to the binding energy, E_b^{SIC} , is only $6136-3342-2790 = 4$ meV for $\text{OH}^-(\text{H}_2\text{O})$, too small to provide a significant correction to the SCAN@FLOSIC overbinding, but it is $5441-2599-2790 = 52$ meV for $\text{H}_3\text{O}^+(\text{H}_2\text{O})$, where it provides

a much more significant correction. This happens despite the lowering of the energy of $\text{H}_3\text{O}^+(\text{H}_2\text{O})$ due to the transfer of a pair of electrons from lone-pair to bond-pair FLOs when the strong hydrogen bond forms in that cationic cluster. Thus the FLOSIC–SCAN method still lacks the balance required to

TABLE III. FLOSIC–SCAN self-interaction correction to the SCAN@FLOSIC total energy, defined as the correction from Eq. (1) to the SCAN total energy evaluated on FLOSIC–SCAN Fermi–Löwdin orbitals, and its contributions from core, bond-pair, and lone-pair electrons. The pair contributions are written in the form $n \times \epsilon$, where n is the number of pairs and ϵ is the average SIC energy of a pair.

System	Energy (meV)			
	Total	Core	Bond-pair	Lone-pair
OH^-	3342	1×251	1×600	3×830
H_2O	2790	1×242	2×545	2×729
H_3O^+	2599	1×277	3×535	1×717
$\text{OH}^-(\text{H}_2\text{O})$	6136	2×245	3×604	5×767
$\text{H}_3\text{O}^+(\text{H}_2\text{O})$	5441	2×251	6×576	2×742

treat both OH^- and $\text{OH}^-(\text{H}_2\text{O})$ accurately enough to capture SIC as needed. The description of H_3O^+ and $\text{H}_3\text{O}^+(\text{H}_2\text{O})$ with FLOSIC is much better in this regard, leading to a significant improvement in the binding of $\text{H}_3\text{O}^+(\text{H}_2\text{O})$.

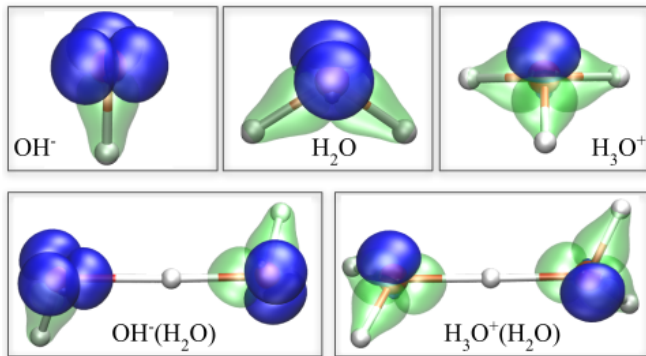


FIG. 6. Isosurfaces ($0.02 e/\text{\AA}^3$) of FLO densities from FLOSIC–SCAN for OH^- , H_2O , H_3O^+ , $\text{OH}^-(\text{H}_2\text{O})$, and $\text{H}_3\text{O}^+(\text{H}_2\text{O})$, showing lone-orbitals in blue and bond-orbitals in green.

C. Water–Halide Ion Interactions

In this section, we explore the interaction energy of water–halide dimers and trimers, each cluster containing one of the three halide anions, F^- , Cl^- , and Br^- . As shown in Fig. 2(a), when the halide anion interacts with one H_2O molecule, the global minimum structures contain one hydrogen bond, in which a halide anion accepts HBs from a donor hydrogen. With increasing size of the anion, the length of the HB increases from 1.39 Å in $\text{F}^-(\text{H}_2\text{O})$ to 2.37 Å in $\text{Br}^-(\text{H}_2\text{O})$, and the HB angle moves away from linearity, indicating a systematic weakening of HBs with the size of anions.

Table IV shows the binding energies of halide–water clusters and the mean unsigned errors (MUEs) obtained with XC functionals in comparison to CCSD(T)/F12b reference energies¹⁷. The reference values show that the magnitudes of the binding energies decrease by $\sim 50\%$ from lighter to heav-

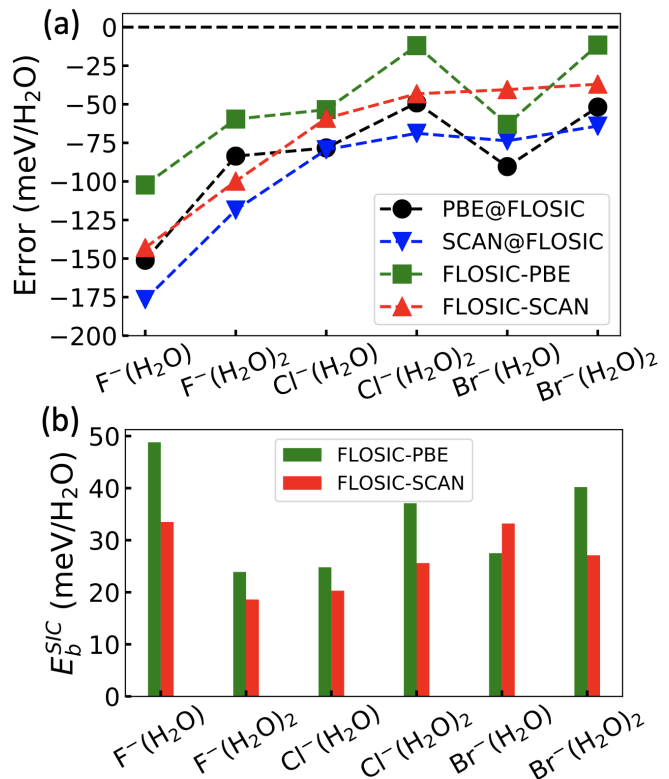


FIG. 7. (a) Error in the binding energies and (b) self-interaction correction to the binding energies (E_b^{SIC}) of $\text{X}^-(\text{H}_2\text{O})_n$ with $\text{X}=\text{F}, \text{Cl}, \text{Br}$ and $n=1,2$ with various functionals compared to the CCSD(T)–F12b reference.

ier halide ions. This trend is qualitatively reproduced by all XC functionals, and follows from the increasing ionic radii from F^- to Br^- . Here, too, FLOSIC–DFA methods systematically reduce the error in binding energies compared to the corresponding parent DFAs. LSDA@FLOSIC predicts too large MUE (302 meV/ H_2O) and FLOSIC–LSDA largely reduces the errors but still displays a large MUE of 184 meV/ H_2O . Both PBE@FLOSIC and SCAN@FLOSIC bring significant improvements compared to LSDA by bringing the MUE below 100 meV/ H_2O . FLOSIC–SCAN predicts an MUE of 70 meV/ H_2O , reducing it by 27 meV/ H_2O from SCAN@FLOSIC. Again, FLOSIC–PBE provides the best agreement with the reference binding energies, predicting on average 50 meV/ H_2O too-strong binding, after reducing the error by 34 meV/ H_2O from PBE@FLOSIC.

Figure 7(a) further illustrates that the error in binding energies decreases with cluster size in all functionals. The SIC contribution to the binding energy is in the range of 25–50 meV/ H_2O with FLOSIC–PBE and 20–35 meV/ H_2O with FLOSIC–SCAN, as shown in Fig. 7(b). Except for $\text{Br}^-(\text{H}_2\text{O})$, FLOSIC–PBE performs better than FLOSIC–SCAN for all water–halide clusters.

TABLE IV. Binding energies with density functionals and the corresponding mean unsigned errors (MUEs) computed with respect to CCSD(T)-F12b reference⁸⁷ for halide-water clusters. The final column shows the percent error (PE) for FLOSIC–PBE. The energies are obtained with the basis DFO* for LSDA, PBE, and SCAN, and with *diffuse-3* for all other functionals.

Cluster	Binding Energy per H ₂ O (meV/H ₂ O)										PE
	Ref.	LSDA	LSDA@ FLOSIC	FLOSIC– LSDA	PBE	PBE@ FLOSIC	FLOSIC– PBE	SCAN	SCAN@ FLOSIC	FLOSIC– SCAN	FLOSIC– PBE
F [−] (H ₂ O)	-1188	-1647	-1638	-1484	-1350	-1339	-1290	-1366	-1364	-1331	8.6 %
Cl [−] (H ₂ O)	-645	-900	-918	-802	-730	-724	-699	-720	-725	-704	8.3 %
Br [−] (H ₂ O)	-556	-785	-811	-669	-634	-646	-619	-624	-630	-596	11.3 %
F [−] (H ₂ O) ₂	-1056	-1398	-1394	-1294	-1142	-1140	-1116	-1174	-1175	-1156	5.6 %
Cl [−] (H ₂ O) ₂	-648	-901	-903	-804	-699	-697	-660	-717	-717	-691	1.9 %
Br [−] (H ₂ O) ₂	-575	-814	-816	-717	-625	-626	-586	-640	-639	-612	2.0 %
MUE	–	296	302	184	85	84	50	96	97	70	–

TABLE V. Binding energies with density functionals and the corresponding mean unsigned errors (MUEs) computed with respect to CCSD(T)-F12b reference⁸⁷ for alkali-water clusters. The final column shows the percent error (PE) for FLOSIC–PBE. The energies are obtained with the basis DFO* for all functionals.

Cluster	Binding Energy (meV/H ₂ O)										PE
	Ref.	LSDA	LSDA@ FLOSIC	FLOSIC– LSDA	PBE	PBE@ FLOSIC	FLOSIC– PBE	SCAN	SCAN@ FLOSIC	FLOSIC– SCAN	FLOSIC– PBE
Li ⁺ (H ₂ O)	-1508	-1619	-1651	-1707	-1502	-1531	-1596	-1472	-1488	-1557	5.8 %
Na ⁺ (H ₂ O)	-1049	-1160	-1185	-1213	-1035	-1048	-1097	-1062	-1072	-1127	4.5 %
K ⁺ (H ₂ O)	-779	-867	-887	-906	-731	-749	-794	-762	-771	-823	1.9 %
Li ⁺ (H ₂ O) ₂	-1404	-1500	-1527	-1581	-1392	-1418	-1481	-1371	-1384	-1443	5.5 %
Na ⁺ (H ₂ O) ₂	-993	-1095	-1115	-1146	-978	-992	-1043	-1003	-1012	-1065	5.0 %
K ⁺ (H ₂ O) ₂	-734	-814	-824	-834	-689	-704	-729	-718	-726	-761	-0.7 %
MUE	–	98	120	153	23	17	47	21	16	51	–

D. Water–Alkali Ion Interactions

In this section, we explore the interaction energy of water–alkali cation dimers and trimers, each cluster containing one of the three alkali cations, Li⁺, Na⁺, and K⁺. The nature of interactions in the global minimum structures of the small water–alkali clusters is different from all the other clusters discussed so far. The water–alkali interaction is not due to HBs, but ion–dipole interactions, in which a cation sits close to a more electronegative oxygen atom, as shown in Fig. 2(b). With the increasing size of the cation, the oxygen–cation distance increases from 1.84 Å in Li⁺(H₂O) to 2.60 Å in K⁺(H₂O), indicating weakening of the binding energy. Table V shows the binding energies of alkali–water clusters and the MUEs obtained with XC functionals in comparison to the CCSD(T)/F12b reference⁸⁷. The reference binding energies show that the binding energies are reduced by ~50% from the lighter (Li⁺) to the heavier (K⁺) alkali ion, and the binding per molecule decreases with an increasing number of H₂O molecules in the cluster. Both of these trends are qualitatively reproduced by all XC functionals. Unlike the results found in the hydrogen-bonded clusters, the FLOSIC–DFA functionals do not improve the binding energies of alkali–water clusters compared to the parent DFAs. The MUEs from FLOSIC–DFA functionals are 30–35 meV/H₂O worse than the corresponding DFAs. Both PBE@FLOSIC and SCAN@FLOSIC predict ~16 meV/H₂O MUE, which is the lowest among all functionals.

Fig. 8 (a) shows the error in binding energies for different clusters. With PBE@FLOSIC, the magnitudes of the binding energies are overestimated in the lighter Li⁺(H₂O) cluster and underestimated in the heavier cation K⁺(H₂O) cluster. In the case of SCAN@FLOSIC, the errors tend to decrease from the lighter to the heavier cation cluster. Using FLOSIC–PBE and FLOSIC–SCAN, the average E_b^{SIC} is ~50 meV/H₂O, with its magnitude declining towards heavier water–alkali clusters, as shown in Fig. 8(b).

For the water–alkali clusters, unlike the other clusters studied here, self-interaction errors seem to be unimportant.

IV. CONCLUSIONS

We have assessed the accuracy of the orbital-by-orbital PZ self-interaction correction²⁶ computed within the FLOSIC methodology³⁶ for the interaction energies between water molecules and various ions, namely, hydroxide, hydronium, halide anions, and alkali cations in gas-phase clusters. These clusters are primarily hydrogen-bonded, except the water–alkali clusters which are bound by ion–dipole interactions. It is known that negatively-charged clusters are subject to erroneous delocalization of the electron density due to self-interaction present in approximate XC functionals such as local and semi-local DFAs. We have employed FLOSIC–DFA methods, where the DFAs are LSDA, PBE, and SCAN, to mitigate this error in the electron density and in the corresponding

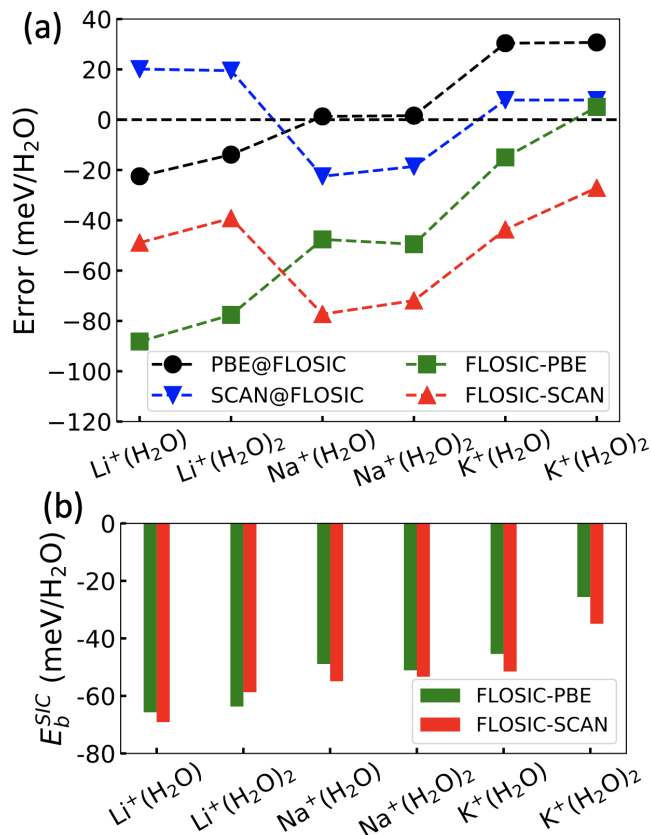


FIG. 8. (a) Error in the binding energies and (b) self-interaction correction to the binding energies (E_b^{SIC}) of $M^+(\text{H}_2\text{O})_n$ ($M=\text{Li}, \text{Na}, \text{K}$) and $n=1,2$ with various functionals compared to the CCSD(T)-F12b.

energetics. The self-interaction corrected density is utilized to quantify the density-driven error in the energies obtained with these DFAs. We have found that the magnitude of the density-driven error increases with diffuse Gaussian functions, which makes the energy convergence of anions with respect to basis functions more ambiguous. The density-driven error is not significant in cations. The self-interaction corrected density allows a meaningful basis-set convergence study for anions with LSDA, PBE, and SCAN. The DFA energies computed here with the *diffuse-3* basis at the FLOSIC-DFA densities, *i.e.*, DFA@FLOSIC, provide an accurate assessment of the accuracy of these functionals for anions.

Fig. 9 shows the summary and cross-comparison of the accuracy of the methods for the four types of water-ion clusters. The DFA@FLOSIC energies show a significant overestimation of the binding energies for the hydrogen-bonded clusters, *i.e.*, protonated water, deprotonated water, and halide-water clusters. The MUE is very large in LSDA@FLOSIC (>300 meV/H₂O) and is significantly reduced in PBE@FLOSIC (54–84 meV/H₂O) and SCAN@FLOSIC (85–98 meV/H₂O). The removal of SIE weakens the binding in hydrogen-bonded clusters and shifts the binding energies toward the accurate references. Surprisingly, the average reduction of the SIE is larger in the binding of protonated water clusters than in deprotonated and water-halide clusters. Because of that, all

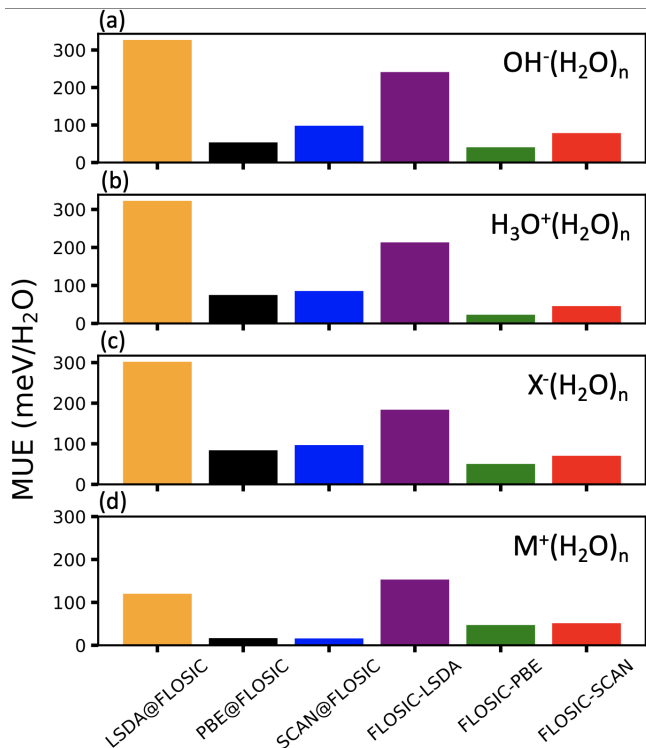


FIG. 9. Mean unsigned error (MUE) given by different functionals for (a) deprotonated water, (b) protonated water, (c) water-halide, and (d) water-alkali clusters, shown from the top to the bottom.

FLOSIC-DFA functionals produce much smaller MUE for the protonated water clusters than for the other hydrogen-bonded clusters. FLOSIC-SCAN predicts the MUE in the range of 46–78 meV/H₂O. FLOSIC-PBE provides the most accurate description of the hydrogen-bonded clusters, with the MUE in the range of 23–47 meV/H₂O. The effect of removing SIE in water-alkali clusters is in stark contrast to that in hydrogen-bonded clusters. Self-interaction correction strengthens the binding of the alkali-water clusters, and as a result, the MUE from FLOSIC-DFAs are worse than the corresponding DFAs. This is in line with the fact that, in other situations, PZ-SIC reduces self-interaction errors but introduces other errors for many-electron densities⁴⁴, as discussed in the next paragraph.

Although FLOSIC-DFAs improve the description of the hydrogen-bonded clusters, the overall results suggest that the PZ SIC method needs improvement in order to achieve more accurate binding energies, in particular, for the small hydrogen-bonded clusters and the alkali-water clusters. The PZ SIC approach is exact for all one-electron densities, however, it is not so accurate in diverse many-electron regions^{89,90}. An appropriate scaling of the PZ SIC is still required to make it equally accurate in many-electron regions. A scaling method that would enhance the SIC contribution to the binding of OH⁻(H₂O) and H₃O⁺(H₂O) clusters and simultaneously reduce the SIC contribution to the binding of water-alkali clusters is highly sought after. A few approaches that locally scale down the PZ SIC have been introduced re-

cently^{90–93}, but more development is needed. The scaled methods have not yet been implemented self-consistently. When implemented on FLOSIC-LSDA FLO densities, the methods of Refs. 90 and 93 improve many calculated properties over PZ SIC, including the energies of the stronger bonds^{47,90–93}, but seriously underbind⁹³ typical hydrogen- and van der Waals-bonded complexes. Our current study with self-consistent FLOSIC implementations of unscaled PZ SIC shows the importance of mitigating the self-interaction error from the electron density and the corresponding energetics in water-ion interactions. We aim to increase the accuracy of self-interaction correction in future works.

SUPPLEMENTARY MATERIAL

The supplementary material includes the optimized FOD coordinates, NRLMOL inputs, and total energies with all methods for the purpose of data reproduction.

ACKNOWLEDGMENTS

This work was supported by the U.S. Department of Energy, Office of Science, Office of Basic Energy Sciences under award number DE-SC0018331 as a part of the Computational Chemical Sciences Program. The work of K.W. and P.B. was supported by the U.S. National Science Foundation under Grant No. DMR-1939528. Calculations for this work were done on Temple University’s HPC resources and thus were supported in part by the National Science Foundation grant number 1625061 and by the US Army Research Laboratory under contract number W911NF-16-2-0189. K.W., B.S., and J.P.P. acknowledge Francesco Paesani and Colin Egan for providing CCSD(T) reference binding energies for halide-water and alkali-water clusters.

DATA AVAILABILITY

The data that support the findings of this study are available within the article and its supplementary material and from the authors upon reasonable request.

- ¹M. Meot-Ner (Mautner), “The Ionic Hydrogen Bond,” *Chem. Rev.* **105**, 213–284 (2005).
- ²K. Sharkas, K. Wagle, B. Santra, S. Akter, R. R. Zope, T. Baruah, K. A. Jackson, J. P. Perdew, and J. E. Peralta, “Self-interaction error overbinds water clusters but cancels in structural energy differences,” *Proc. Natl. Acad. Sci.* **117**, 11283–11288 (2020).
- ³M. Chen, H.-Y. Ko, R. C. Remsing, M. F. Calegari Andrade, B. Santra, Z. Sun, A. Selloni, R. Car, M. L. Klein, J. P. Perdew, and X. Wu, “Ab initio theory and modeling of water,” *Proc. Natl. Acad. Sci.* **114**, 10846–10851 (2017).
- ⁴N. F. A. van der Vegt, K. Haldrup, S. Roke, J. Zheng, M. Lund, and H. J. Bakker, “Water-Mediated Ion Pairing: Occurrence and Relevance,” *Chem. Rev.* **116**, 7626–7641 (2016).
- ⁵H. Ohtaki and T. Radnai, “Structure and dynamics of hydrated ions,” *Chem. Rev.* **93**, 1157–1204 (1993).
- ⁶Y. Marcus, “Effect of Ions on the Structure of Water: Structure Making and Breaking,” *Chem. Rev.* **109**, 1346–1370 (2009).

- ⁷N. Agmon, H. J. Bakker, R. K. Campen, R. H. Henchman, P. Pohl, S. Roke, M. Thämer, and A. Hassanali, “Protons and Hydroxide Ions in Aqueous Systems,” *Chem. Rev.* **116**, 7642–7672 (2016).
- ⁸W. Kohn and L. J. Sham, “Self-consistent equations including exchange and correlation effects,” *Phys. Rev.* **140**, A1133–A1138 (1965).
- ⁹D. Marx, M. E. Tuckerman, J. Hutter, and M. Parrinello, “The nature of the hydrated excess proton in water,” *Nature* **397**, 601–604 (1999).
- ¹⁰P. L. Geissler, C. Dellago, D. Chandler, J. Hutter, and M. Parrinello, “Autotization in liquid water,” *Science* **291**, 2121–2124 (2001).
- ¹¹M. E. Tuckerman, D. Marx, and M. Parrinello, “The nature and transport mechanism of hydrated hydroxide ions in aqueous solution,” *Nature* **417**, 925–929 (2002).
- ¹²M. Chen, L. Zheng, B. Santra, H.-Y. Ko, R. A. DiStasio Jr, M. L. Klein, R. Car, and X. Wu, “Hydroxide diffuses slower than hydronium in water because its solvated structure inhibits correlated proton transfer,” *Nat. Chem.* **10**, 413–419 (2018).
- ¹³R. A. DiStasio, B. Santra, Z. Li, X. Wu, and R. Car, “The individual and collective effects of exact exchange and dispersion interactions on the ab initio structure of liquid water,” *J. Chem. Phys.* **141**, 084502 (2014).
- ¹⁴B. Santra, R. A. DiStasio, F. Martelli, and R. Car, “Local structure analysis in ab initio liquid water,” *Mol. Phys.* **113**, 2829–2841 (2015).
- ¹⁵A. Bankura, B. Santra, R. A. DiStasio, C. W. Swartz, M. L. Klein, and X. Wu, “A systematic study of chloride ion solvation in water using van der Waals inclusive hybrid density functional theory,” *Mol. Phys.* **113**, 2842–2854 (2015).
- ¹⁶J. Wang, G. Román-Pérez, J. M. Soler, E. Artacho, and M.-V. Fernández-Serra, “Density, structure, and dynamics of water: The effect of van der waals interactions,” *J. Chem. Phys.* **134**, 024516 (2011).
- ¹⁷C. K. Egan, B. B. Bizzarro, M. Riera, and F. Paesani, “Nature of Alkali Ion–Water Interactions: Insights from Many-Body Representations and Density Functional Theory. II,” *J. Chem. Theory Comput.* **16**, 3055–3072 (2020).
- ¹⁸C. K. Egan and F. Paesani, “Assessing Many-Body Effects of Water Self-Ions. I: OH⁻(H₂O)_n Clusters,” *J. Chem. Theory Comput.* **14**, 1982–1997 (2018).
- ¹⁹C. K. Egan and F. Paesani, “Assessing Many-Body Effects of Water Self-Ions. II: H₃O⁺(H₂O)_n Clusters,” *J. Chem. Theory Comput.* **15**, 4816–4833 (2019).
- ²⁰F. Paesani, P. Bajaj, and M. Riera, “Chemical accuracy in modeling halide ion hydration from many-body representations,” *Adv. Phys. X* **4**, 1631212 (2019).
- ²¹B. B. Bizzarro, C. K. Egan, and F. Paesani, “Nature of Halide–Water Interactions: Insights from Many-Body Representations and Density Functional Theory,” *J. Chem. Theory Comput.* **15**, 2983–2995 (2019).
- ²²M. J. Gillan, D. Alfè, and A. Michaelides, “Perspective: How good is dft for water?” *J. Chem. Phys.* **144**, 130901 (2016).
- ²³B. Santra, A. Michaelides, M. Fuchs, A. Tkatchenko, C. Filippi, and M. Scheffler, “On the accuracy of density-functional theory exchange-correlation functionals for H bonds in small water clusters. II. The water hexamer and van der Waals interactions,” *J. Chem. Phys.* **129**, 194111 (2008).
- ²⁴J. Sun, A. Ruzsinszky, and J. P. Perdew, “Strongly constrained and appropriately normed semilocal density functional,” *Phys. Rev. Lett.* **115**, 036402 (2015).
- ²⁵J. Sun, R. C. Remsing, Y. Zhang, Z. Sun, A. Ruzsinszky, H. Peng, Z. Yang, A. Paul, U. Waghmare, X. Wu, M. L. Klein, and J. P. Perdew, “Accurate first-principles structures and energies of diversely bonded systems from an efficient density functional,” *Nat. Chem.* **8**, 831–836 (2016).
- ²⁶J. P. Perdew and A. Zunger, “Self-interaction correction to density-functional approximations for many-electron systems,” *Phys. Rev. B* **23**, 5048–5079 (1981).
- ²⁷H. B. Shore, J. H. Rose, and E. Zaremba, “Failure of the local exchange approximation in the evaluation of the H⁻ ground state,” *Phys. Rev. B* **15**, 2858–2861 (1977).
- ²⁸N. Rösch and S. B. Trickey, “Comment on “Concerning the applicability of density functional methods to atomic and molecular negative ions” [J. Chem. Phys. 105, 862 (1996)],” *J. Chem. Phys.* **106**, 8940–8941 (1997).
- ²⁹J. C. Rienstra-Kiracofe, G. S. Tschumper, H. F. Schaefer, S. Nandi, and G. B. Ellison, “Atomic and Molecular Electron Affinities: Photoelectron Experiments and Theoretical Computations,” *Chem. Rev.* **102**, 231–282

- (2002).
- ³⁰F. Jensen, "Describing Anions by Density Functional Theory: Fractional Electron Affinity," *J. Chem. Theory Comput.* **6**, 2726–2735 (2010).
- ³¹M.-C. Kim, E. Sim, and K. Burke, "Communication: Avoiding unbound anions in density functional calculations," *J. Chem. Phys.* **134**, 171103 (2011).
- ³²A. Wasserman, J. Nafziger, K. Jiang, M.-C. Kim, E. Sim, and K. Burke, "The Importance of Being Inconsistent," *Annu. Rev. Phys. Chem.* **68**, 555–581 (2017).
- ³³A. Ruzsinszky, J. P. Perdew, G. I. Csonka, O. A. Vydrov, and G. E. Scuseria, "Spurious fractional charge on dissociated atoms: Pervasive and resilient self-interaction error of common density functionals," *J. Chem. Phys.* **125**, 194112 (2006).
- ³⁴B. Santra, A. Michaelides, and M. Scheffler, "Coupled cluster benchmarks of water monomers and dimers extracted from density-functional theory liquid water: The importance of monomer deformations," *J. Chem. Phys.* **131**, 124509 (2009).
- ³⁵M. R. Pederson, A. Ruzsinszky, and J. P. Perdew, "Communication: Self-interaction correction with unitary invariance in density functional theory," *J. Chem. Phys.* **140**, 121103 (2014).
- ³⁶Z.-H. Yang, M. R. Pederson, and J. P. Perdew, "Full self-consistency in the fermi-orbital self-interaction correction," *Phys. Rev. A* **95**, 052505 (2017).
- ³⁷M. R. Pederson, R. A. Heaton, and C. C. Lin, "Density-functional theory with self-interaction correction: Application to the lithium molecule," *J. Chem. Phys.* **82**, 2688–2699 (1985).
- ³⁸O. A. Vydrov and G. E. Scuseria, "Effect of the Perdew–Zunger self-interaction correction on the thermochemical performance of approximate density functionals," *J. Chem. Phys.* **121**, 8187 (2004).
- ³⁹M. R. Pederson, T. Baruah, D. Y. Kao, and L. Basurto, "Self-interaction corrections applied to Mg-porphyrin, C₆₀, and pentacene molecules," *J. Chem. Phys.* **144**, 164117 (2016).
- ⁴⁰T. Hahn, S. Schwalbe, J. Kortus, and M. R. Pederson, "Symmetry Breaking within Fermi–Löwdin Orbital Self-Interaction Corrected Density Functional Theory," *J. Chem. Theory Comput.* **13**, 5823–5828 (2017).
- ⁴¹D. Y. Kao, K. Withanage, T. Hahn, J. Batool, J. Kortus, and K. Jackson, "Self-consistent self-interaction corrected density functional theory calculations for atoms using Fermi–Löwdin orbitals: Optimized Fermi-orbital descriptors for Li–Kr," *J. Chem. Phys.* **147** (2017), 10.1063/1.4996498.
- ⁴²K. Sharkas, L. Li, K. Trepte, K. P. K. Withanage, R. P. Joshi, R. R. Zope, T. Baruah, J. K. Johnson, K. A. Jackson, and J. E. Peralta, "Shrinking self-interaction errors with the fermi–löwdin orbital self-interaction-corrected density functional approximation," *J. Phys. Chem. A* **122**, 9307–9315 (2018).
- ⁴³R. P. Joshi, K. Trepte, K. P. K. Withanage, K. Sharkas, Y. Yamamoto, L. Basurto, R. R. Zope, T. Baruah, K. A. Jackson, and J. E. Peralta, "Fermi–Löwdin orbital self-interaction correction to magnetic exchange couplings," *J. Chem. Phys.* **149**, 164101 (2018).
- ⁴⁴C. Shahi, P. Bhattarai, K. Wagle, B. Santra, S. Schwalbe, T. Hahn, J. Kortus, K. A. Jackson, J. E. Peralta, K. Trepte, S. Lehtola, N. K. Nepal, H. Myneni, B. Neupane, S. Adhikari, A. Ruzsinszky, Y. Yamamoto, T. Baruah, R. R. Zope, and J. P. Perdew, "Stretched or noded orbital densities and self-interaction correction in density functional theory," *J. Chem. Phys.* **150**, 174102 (2019).
- ⁴⁵A. I. Johnson, K. P. K. Withanage, K. Sharkas, Y. Yamamoto, T. Baruah, R. R. Zope, J. E. Peralta, and K. A. Jackson, "The effect of self-interaction error on electrostatic dipoles calculated using density functional theory," *J. Chem. Phys.* **151**, 174106 (2019).
- ⁴⁶K. P. K. Withanage, S. Akter, C. Shahi, R. P. Joshi, C. Diaz, Y. Yamamoto, R. Zope, T. Baruah, J. P. Perdew, J. E. Peralta, and K. A. Jackson, "Self-interaction-free electric dipole polarizabilities for atoms and their ions using the Fermi–Löwdin self-interaction correction," *Phys. Rev. A* **100**, 012505 (2019).
- ⁴⁷L. Li, K. Trepte, K. A. Jackson, and J. K. Johnson, "Application of Self-Interaction Corrected Density Functional Theory to Early, Middle, and Late Transition States," *J. Phys. Chem. A* **124**, 8223–8234 (2020).
- ⁴⁸S. Adhikari, B. Santra, S. Ruan, P. Bhattarai, N. K. Nepal, K. A. Jackson, and A. Ruzsinszky, "The Fermi–Löwdin self-interaction correction for ionization energies of organic molecules," *J. Chem. Phys.* **153**, 184303 (2020).
- ⁴⁹J. Vargas, P. Ufondu, T. Baruah, Y. Yamamoto, K. A. Jackson, and R. R. Zope, "Importance of self-interaction-error removal in density functional calculations on water cluster anions," *Phys. Chem. Chem. Phys.* **22**, 3789–3799 (2020).
- ⁵⁰S. Akter, Y. Yamamoto, C. M. Diaz, K. A. Jackson, R. R. Zope, and T. Baruah, "Study of self-interaction errors in density functional predictions of dipole polarizabilities and ionization energies of water clusters using Perdew–Zunger and locally scaled self-interaction corrected methods," *J. Chem. Phys.* **153**, 164304 (2020).
- ⁵¹J. Batool, T. Hahn, and M. R. Pederson, "Magnetic Signatures of Hydroxyl- and Water-Terminated Neutral and Tetra-Anionic Mn 12 -Acetate," *J. Comput. Chem.* **40**, 2301–2308 (2019).
- ⁵²J. P. Perdew, M. Ernzerhof, and K. Burke, "Rationale for mixing exact exchange with density functional approximations," *J. Chem. Phys.* **105**, 9982 (1996).
- ⁵³V. S. Bryantsev, M. S. Diallo, A. C. T. van Duin, and W. A. Goddard, "Evaluation of b3lyp, x3lyp, and m06-class density functionals for predicting the binding energies of neutral, protonated, and deprotonated water clusters," *J. Chem. Theory Comput.* **5**, 1016–1026 (2009).
- ⁵⁴M. R. Pederson and K. A. Jackson, "Variational mesh for quantum-mechanical simulations," *Phys. Rev. B* **41**, 7453 (1990).
- ⁵⁵*FLOSIC code public release* (accessed November 4, 2019), <https://github.com/FLOSIC/PublicRelease>.
- ⁵⁶K. Jackson and M. R. Pederson, "Accurate forces in a local-orbital approach to the local-density approximation," *Phys. Rev. B* **42**, 3276–3281 (1990).
- ⁵⁷M. R. Pederson and K. A. Jackson, "Pseudopotentials for simulations on metallic systems," *Phys. Rev. B* **43**, 7312–7315 (1991).
- ⁵⁸D. Porezag and M. R. Pederson, "Infrared intensities and raman-scattering activities within density-functional theory," *Phys. Rev. B* **54**, 7830–7836 (1996).
- ⁵⁹A. Briley, M. R. Pederson, K. A. Jackson, D. C. Patton, and D. V. Porezag, "Vibrational frequencies and intensities of small molecules: All-electron, pseudopotential, and mixed-potential methodologies," *Phys. Rev. B* **58**, 1786–1793 (1998).
- ⁶⁰M. Pederson, D. Porezag, J. Kortus, and D. Patton, "Strategies for Massively Parallel Local-Orbital-Based Electronic Structure Methods," *Phys. status solidi* **217**, 197–218 (2000).
- ⁶¹D. Porezag and M. R. Pederson, "Optimization of gaussian basis sets for density-functional calculations," *Phys. Rev. A* **60**, 2840–2847 (1999).
- ⁶²J. C. Slater, "A simplification of the hartree-fock method," *Phys. Rev.* **81**, 385–390 (1951).
- ⁶³J. P. Perdew and Y. Wang, "Accurate and simple analytic representation of the electron-gas correlation energy," *Phys. Rev. B* **45**, 13244–13249 (1992).
- ⁶⁴J. P. Perdew, K. Burke, and M. Ernzerhof, "Generalized gradient approximation made simple," *Phys. Rev. Lett.* **77**, 3865–3868 (1996).
- ⁶⁵Y. Yamamoto, C. M. Diaz, L. Basurto, K. A. Jackson, T. Baruah, and R. R. Zope, "Fermi–Löwdin orbital self-interaction correction using the strongly constrained and appropriately normed meta-GGA functional," *J. Chem. Phys.* **151**, 154105 (2019).
- ⁶⁶M. R. Pederson and C. C. Lin, "Localized and canonical atomic orbitals in self-interaction corrected local density functional approximation," *J. Chem. Phys.* **88**, 1807–1817 (1988).
- ⁶⁷W. L. Luken and D. N. Beratan, "Localized orbitals and the fermi hole," *Theo. Chim. Acta.* **61**, 265–281 (1982).
- ⁶⁸W. L. Luken and J. C. Culbertson, "Localized orbitals based on the fermi hole," *Theo. Chim. Acta.* **66**, 279–293 (1984).
- ⁶⁹P. Löwdin, "On the non-orthogonality problem connected with the use of atomic wave functions in the theory of molecules and crystals," *J. Chem. Phys.* **18**, 365–375 (1950).
- ⁷⁰S. Schwalbe, K. Trepte, L. Fiedler, A. I. Johnson, J. Kraus, T. Hahn, J. E. Peralta, K. A. Jackson, and J. Kortus, "Interpretation and Automatic Generation of Fermi-Orbital Descriptors," *J. Comput. Chem.* **40**, 2843–2857 (2019).
- ⁷¹M. R. Pederson, "Fermi orbital derivatives in self-interaction corrected density functional theory: Applications to closed shell atoms," *J. Chem. Phys.* **142**, 064112 (2015).
- ⁷²M. Pederson and T. Baruah, "Self-interaction corrections within the fermi-orbital-based formalism," in *Advances In Atomic, Molecular, and Optical Physics*, Vol. 64, edited by E. Arimondo, C. C. Lin, and S. F. Yeli (Academic Press, Burlington, 2015) pp. 153–180.
- ⁷³T. Hahn, S. Liebing, J. Kortus, and M. R. Pederson, "Fermi orbital self-interaction corrected electronic structure of molecules beyond local density

- approximation," *J. Chem. Phys.* **143**, 224104 (2015).
- ⁷⁴K. A. Jackson, J. E. Peralta, R. P. Joshi, K. P. Withanage, K. Trepte, K. Sharkas, and A. I. Johnson, "Towards efficient density functional theory calculations without self-interaction: The fermi-löwdin orbital self-interaction correction," *J. Phys. Conf. Ser* **1290**, 012002 (2019).
- ⁷⁵C. G. Broyden, "The Convergence of a Class of Double-rank Minimization Algorithms I. General Considerations," *IMA J. Appl. Math.* **6**, 76–90 (1970).
- ⁷⁶R. Fletcher, "A new approach to variable metric algorithms," *Comput. J.* **13**, 317–322 (1970).
- ⁷⁷D. Goldfarb, "A family of variable-metric methods derived by variational means," *Math. Comput.* **24**, 23–23 (1970).
- ⁷⁸D. F. Shanno, "Conditioning of quasi-Newton methods for function minimization," *Math. Comput.* **24**, 647–647 (1970).
- ⁷⁹M.-C. Kim, E. Sim, and K. Burke, "Understanding and Reducing Errors in Density Functional Calculations," *Phys. Rev. Lett.* **111**, 073003 (2013).
- ⁸⁰M.-C. Kim, H. Park, S. Son, E. Sim, and K. Burke, "Improved DFT Potential Energy Surfaces via Improved Densities," *J. Phys. Chem. Lett.* **6**, 3802–3807 (2015).
- ⁸¹A. D. Becke, "Density-functional exchange-energy approximation with correct asymptotic behavior," *Phys. Rev. A* **38**, 3098–3100 (1988).
- ⁸²C. Lee, W. Yang, and R. G. Parr, "Development of the colle-salvetti correlation-energy formula into a functional of the electron density," *Phys. Rev. B* **37**, 785–789 (1988).
- ⁸³H.-J. Werner, F. R. Manby, and P. J. Knowles, "Fast linear scaling second-order Møller-Plesset perturbation theory (MP2) using local and density fitting approximations," *J. Chem. Phys.* **118**, 8149–8160 (2003).
- ⁸⁴T. B. Adler, G. Knizia, and H.-J. Werner, "A simple and efficient CCSD(T)-F12 approximation," *J. Chem. Phys.* **127**, 221106 (2007).
- ⁸⁵G. Knizia, T. B. Adler, and H.-J. Werner, "Simplified CCSD(T)-F12 methods: Theory and benchmarks," *J. Chem. Phys.* **130**, 054104 (2009).
- ⁸⁶D. Manna, M. K. Kesharwani, N. Sylvetsky, and J. M. L. Martin, "Conventional and explicitly correlated ab initio benchmark study on water clusters: Revision of the begdb and water27 data sets," *J. Chem. Theory Comput.* **13**, 3136–3152 (2017).
- ⁸⁷D. J. Arismendi-Arrieta, M. Riera, P. Bajaj, R. Prosimiti, and F. Paesani, "i-TTM Model for Ab Initio-Based Ion–Water Interaction Potentials. I. Halide–Water Potential Energy Functions," *J. Phys. Chem. B* **120**, 1822–1832 (2016).
- ⁸⁸L. Goerigk, A. Hansen, C. Bauer, S. Ehrlich, A. Najibi, and S. Grimme, "A look at the density functional theory zoo with the advanced GMTKN55 database for general main group thermochemistry, kinetics and noncovalent interactions," *Phys. Chem. Chem. Phys.* **19**, 32184–32215 (2017).
- ⁸⁹O. A. Vydrov, G. E. Scuseria, J. P. Perdew, A. Ruzsinszky, and G. I. Csonka, "Scaling down the Perdew-Zunger self-interaction correction in many-electron regions," *J. Chem. Phys.* **124**, 094108 (2006).
- ⁹⁰B. Santra and J. P. Perdew, "Perdew-zunger self-interaction correction: How wrong for uniform densities and large-z atoms?" *J. Chem. Phys.* **150**, 174106 (2019).
- ⁹¹R. R. Zope, Y. Yamamoto, C. M. Diaz, T. Baruah, J. E. Peralta, K. A. Jackson, B. Santra, and J. P. Perdew, "A step in the direction of resolving the paradox of Perdew-Zunger self-interaction correction," *J. Chem. Phys.* **151**, 214108 (2019).
- ⁹²P. Bhattarai, K. Wagle, C. Shahi, Y. Yamamoto, S. Romero, B. Santra, R. R. Zope, J. E. Peralta, K. A. Jackson, and J. P. Perdew, "A step in the direction of resolving the paradox of Perdew–Zunger self-interaction correction. II. Gauge consistency of the energy density at three levels of approximation," *J. Chem. Phys.* **152**, 214109 (2020).
- ⁹³P. Bhattarai, B. Santra, K. Wagle, Y. Yamamoto, R. R. Zope, A. Ruzsinszky, K. A. Jackson, and J. P. Perdew, "Exploring and Enhancing the Accuracy of Interior-Scaled Perdew-Zunger Self-Interaction Correction," in preparation.